Evidence for Lattice Effects at the Charge-Ordering Transition in $(TMTTF)_2X$

M. de Souza,[1] P. Foury-Leylekian,[2] A. Moradpour,[2] J.-P. Pouget,[2] and M. Lang[1]

[1]*Physikalisches Institut, Goethe-Universität Frankfurt, SFB/TRR 49, D-60438 Frankfurt(M), Germany*

[2]*Laboratoire de Physique des Solides, Université Paris Sud, CNRS UMR 8502, Orsay, France*

(Received 4 July 2008; published 21 November 2008)

High-resolution thermal expansion measurements have been performed for exploring the mysterious "structureless transition" in $(TMTTF)_2X$ ($X = PF_6$ and AsF_6), where charge ordering at T_{CO} coincides with the onset of ferroelectric order. Particularly distinct lattice effects are found at T_{CO} in the uniaxial expansivity along the interstack $\boldsymbol{c}^*$ direction. We propose a scheme involving a charge modulation along the TMTTF stacks and its coupling to displacements of the counteranions X^-. These anion shifts, which lift the inversion symmetry enabling ferroelectric order to develop, determine the 3D charge pattern without ambiguity. Evidence is found for another anomaly for both materials at $T_{int} \simeq 0.6T_{CO}$ indicative of a phase transition related to the charge ordering.

DOI: 10.1103/PhysRevLett.101.216403 PACS numbers: 71.20.Rv, 65.40.De, 71.30.+h

Charge ordering (CO) has become a main issue for understanding strongly correlated electron systems. Besides its diverse manifestations in transition-metal oxides [1], it is now recognized that the CO phenomena also play a key role for D_2A organic charge-transfer (CT) salts with a variety of donor D and acceptor A molecules, such as $(BEDT\text{-}TTF)_2X$, $(TMTTF)_2X$, and $(DI\text{-}DCNQI)_2Y$ (see [2,3], and references therein). In these soft materials, the CO induces an insulating state, which, by chemical substitution or hydrostatic pressure, can be tuned towards a metallic and low-temperature superconducting phase [4]. The CO transition has been attributed to the importance of both on-site U and nearest-neighbor V Coulomb interactions [5] with influence from electron-lattice coupling [6–8]. However, the definite role of the lattice for charge localization has remained elusive.

Recently, an unexpected CO phase transition has been discovered for the strongly one-dimensional (1D) $(TMTTF)_2X$ salts, preceding the transition into the tetramerized spin-Peierls (SP) ground state. At the transition temperatures $T_{CO} \simeq 65$ ($X = PF_6$) and 105 K (AsF_6) [9], CO coincides with the onset of ferroelectric order [10,11]. This discovery, which shed new light on earlier observations on related materials [12], together with the lack of signatures in the magnetic properties, indicates that here one is dealing with a surprising ferroelectric version of the Mott-Hubbard state [11]. It has been argued that effects of CO can be anticipated also in the more metallic $(TMTSF)_2X$ systems [11] and hence are relevant over wide ranges in the unified phase diagram of $(TM)_2X$ (TM = TMTTF and TMTSF). The mystery surrounding the CO transition, now known as the "structureless transition," arose from the fact that up until now no lattice effects at T_{CO} have been observed [13,14]. This is particularly puzzling as atomic displacements, breaking the inversion symmetry, are a prerequisite for ferroelectricity to occur in these materials.

In this Letter, we report for the first time lattice effects accompanying the CO transition for $(TMTTF)_2X$ by employing thermal expansion measurements. The dilatometer used (built after Ref. [15]) has been particularly suitable for exploring phase transitions in small and fragile crystals of organic CT salts [16] due to its high resolution of $\Delta l/l \sim 10^{-10}$, where l is the sample length.

Measurements have been performed on crystals of $(TMTTF)_2X$ with the centrosymmetric anions $X = AsF_6$ and PF_6. The crystals, grown from THF using the standard procedure, are needle-shaped with dimensions of about $10 \times 1 \times 0.5$ mm^3 with the needle axis parallel to the intrastack $\boldsymbol{a}$ axis. Measurements were conducted along the $\boldsymbol{a}$, $\boldsymbol{b}'$, and $\boldsymbol{c}^*$ axes [17], where $\boldsymbol{b}'$ is perpendicular to the $\boldsymbol{a}$ axis in the $(\boldsymbol{a}, \boldsymbol{b})$ plane and $\boldsymbol{c}^*$ is perpendicular to the $(\boldsymbol{a}, \boldsymbol{b})$ and $(\boldsymbol{a}, \boldsymbol{b}')$ planes. Care was taken to keep the uniaxial stress, exerted by the dilatometer cell on the crystal, below a maximum value of about 0.5 MPa.

In Figs. 1 and 2, we show the results of the uniaxial coefficient of thermal expansion $\alpha_i(T) = l_i^{-1} dl_i/dT$ ($i = a$, b', or c^*) for $X = PF_6$ and AsF_6 below 200 K [18]. The data are dominated by large and anisotropic lattice contributions. However, deviations from an ordinary lattice expansion, characterized by an $\alpha(T)$ which increases monotonically with T (Debye-like), become evident at higher temperatures. Here α_i decreases with increasing temperature, indicating the action of a negative contribution which grows with temperature. This effect is particularly strongly pronounced in α_{c^*} for both salts and larger for the $X = AsF_6$ when compared to the PF_6 salt.

Such a sizable negative contribution is unlikely to originate in electronic degrees of freedom coupled to the lattice. Also, a magnetic contribution α_{mag}, due to 1D spin excitations [20], located at $k_B T^{\alpha} \simeq 0.48J$ [19] (J is the exchange coupling constant), is unlikely as the sign of α_{mag} is given by the pressure dependence of J [21], which is positive here [22]. Rather, the negative contribution may

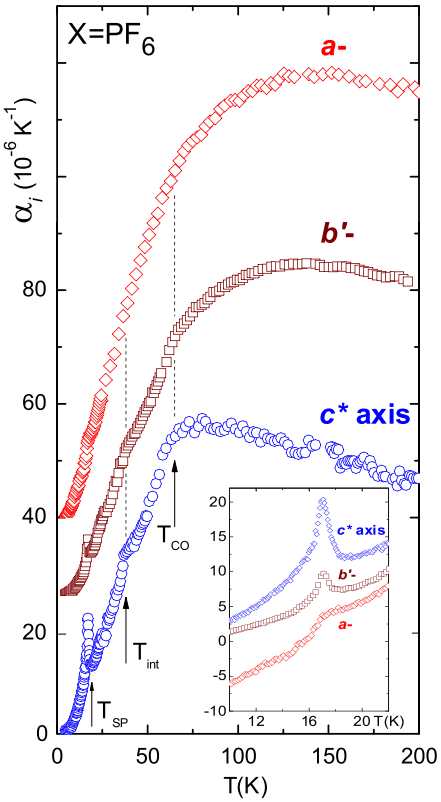

FIG. 1 (color online). Uniaxial expansivities along three orthogonal axes of $(TMTTF)_2PF_6$. The curves have been offset for clarity. Arrows mark the spin-Peierls (T_{SP}) and charge-ordering (T_{CO}) transition temperatures reported in the literature and another transition (T_{int}) revealed here. Broken lines at T_{CO} and T_{int} are guides for the eyes. The inset shows details of the α_i anomalies at T_{SP}.

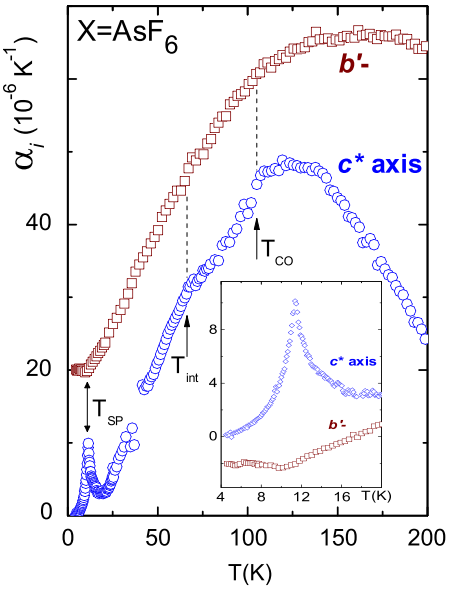

FIG. 2 (color online). Uniaxial expansivities along the $\boldsymbol{b}'$ and $\boldsymbol{c}^*$ axes [17] of $(TMTTF)_2AsF_6$ with phase transition temperatures (arrows) as defined in Fig. 1. The gap in α_{c*} data between 37 and 41 K corresponds to a range of large noise. Curves have been offset for clarity. Broken lines are guides for the eyes. The inset shows details of the anomalies at T_{SP}.

indicate some unusual lattice dynamics. As a possible mechanism, we propose that rotational or translational modes of rigid PF_6 or AsF_6 units linked to the TMTTF molecules via *F-S* halogen bonds cause a negative contribution to α. The size of this contribution is expected to grow with the size of the anion. Indeed, these octahedral anions, trapped in centrosymmetric cavities delimited by the methyl groups [13], are known to be highly disordered at high temperatures and thought to be rotating [23]. As has been discussed in connection with "negative thermal expansion" materials [24], such "rigid-unit modes" may pull the entire structure inwards giving rise to a lattice contraction on thermal excitation.

In addition, the data in Figs. 1 and 2 exhibit distinct, sharp features indicative of phase transitions. Their positions coincide with the transition temperatures into the CO and SP state (arrows labeled T_{CO} and T_{SP} in Figs. 1 and 2) reported in the literature, e.g., Refs. [9,20]. Prominent effects show up at T_{SP} which are most strongly pronounced in α_{c^*} for both salts; cf. the insets of Figs. 1 and 2. A detailed analysis of the phase transition anomalies at T_{SP} will be published elsewhere.

Clear signatures in α_i are also revealed at T_{CO}. The lattice effects accompanying the CO transition constitute the central results of this Letter. The strongest effect is again observed in α_{c^*}, yielding a sharp kink at T_{CO} followed by a rapid reduction immediately below the transition temperature. The anomaly is similar for both salts (cf. Figs. 1 and 2) albeit somewhat more distinct for the AsF_6 system. A corresponding feature, though less strongly pronounced, can be seen also in $\alpha_{b'}$ for $X = PF_6$, whereas it is less evident in $\alpha_{b'}$ for $X = AsF_6$. A still smaller, if any, effect at T_{CO} is found in α_a for PF_6 [17]. We stress that measurements of α_{c^*} on a second $X = PF_6$ crystal yielded practically identical results to those shown in Fig. 1. The anomalous T dependences of α_{c^*} in Figs. 1 and 2 suggest a relation between T_{CO} and the negative thermal expansion contribution: Upon cooling through T_{CO}, this negative contribution vanishes giving way to a positive slope $d\alpha_{c^*}/dT > 0$ for $T < T_{CO}$.

The data in Figs. 1 and 2 disclose yet another anomaly indicative of a phase transition which has been overlooked so far: At an intermediate temperature $T_{int} \simeq (39 \pm 2)$ (PF_6) and (65 ± 2) K (AsF_6), the α_i data for both salts reveal a sharp kink, which is most strongly pronounced in α_{c^*}.

The various anomalies become particularly clear in the volume expansion coefficient $\beta = \alpha_a + \alpha_{b'} + \alpha_{c^*}$, shown in Fig. 3 for the $X = PF_6$ salt as β/T vs T. The data unveil striking similarities in the anomalies at T_{CO} and T_{int}, i.e., sharp kinks accompanied by distinct changes in the slope, indicative of a common nature of both transitions. In fact,

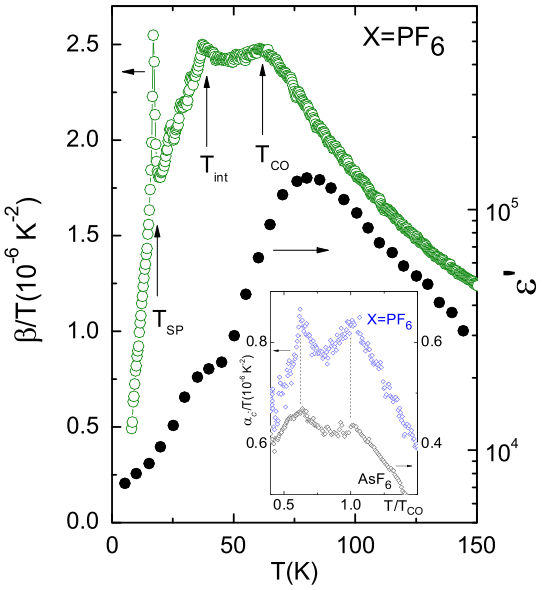

FIG. 3 (color online). Left scale: Volume expansivity $\beta = \alpha_a + \alpha_{b'} + \alpha_{c^*}$ (open circles) as β/T for $(TMTTF)_2PF_6$ determined from the data in Fig. 1. Arrows at T_{SP}, T_{CO}, and T_{int} are defined in Fig. 1. Right scale: Dielectric permittivity ϵ' reproduced from Ref. [25] plotted on the same T scale. Inset: α_{c^*} data for $(TMTTF)_2X$ with $X = PF_6$ (left scale) and $X = AsF_6$ (right scale) as α_{c^*}/T vs T/T_{CO}.

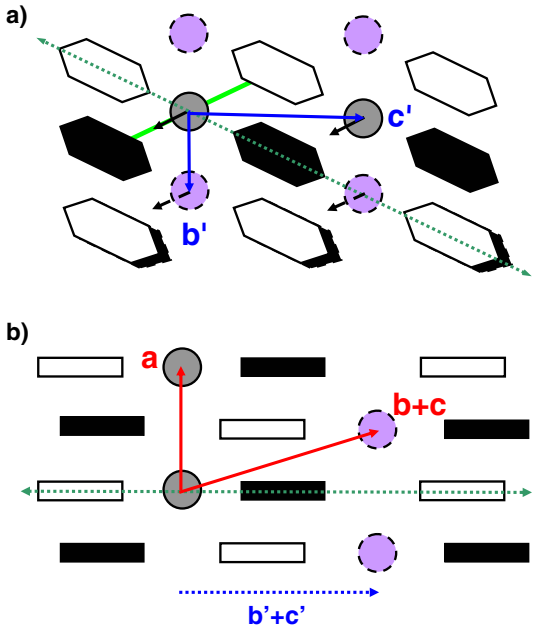

FIG. 4 (color online). (a) Schematic arrangement of TMTTF molecules (hexagons/rectangles) and anions (circles) in the $(\boldsymbol{b}', \boldsymbol{c}')$ plane, i.e., perpendicular to the intrastack $\boldsymbol{a}$ axis, and (b) the $(\boldsymbol{a}, \boldsymbol{b}' + \boldsymbol{c}')$ plane. Green lines exemplarily show short S-F contacts. Black (white) hexagons/rectangles indicate charge $\rho = 0.5 + \delta$ $(0.5 - \delta)$ on the TMTTF molecule in the CO state. Closed and dotted symbols refer to positions within the $(\boldsymbol{b}', \boldsymbol{c}')$ plane and shifted by about $\boldsymbol{a}/2$ along the $\boldsymbol{a}$ axis, respectively. Arrows indicate the proposed shifts of the anions X^- towards the $(TMTTF)^{\rho=0.5+\delta}$ molecules.

an origin of T_{int} related to CO is corroborated by reexamining results of the dielectric permittivity ϵ' for the same salt [11] also shown in Fig. 3. The sharp kink in β/T at T_{int} coincides with a second peak in ϵ' lying on the low-T side of the main ϵ' maximum. We emphasize that the shift in the position of the latter relative to the feature in β is likely due to the frequency dependence in ϵ' observed for this salt [10]. In the inset in Fig. 3, we compare the expansivity results for the $X = PF_6$ with those for the AsF_6 salt by plotting both data sets on a reduced temperature scale T/T_{CO}. Because of the lack of α_a data for the AsF_6 salt [17], the comparison is made for α_{c^*} where the effects are most strongly pronounced. The coincidence in the peak positions, implying T_{int} to scale with T_{CO} for both compounds, suggests that these two features are closely related to each other.

The uniaxial expansivity data in Figs. 1 and 2 provide clear evidence that it is the interstack $\boldsymbol{c}^*$ axis which is most strongly involved in the transition at T_{CO}. The $\boldsymbol{c}^*$ direction is distinct in that it incorporates the anions X: Along $\boldsymbol{c}^*$, $(\boldsymbol{a}, \boldsymbol{b})$ planes of TMTTF molecules alternate with planes of anions X; cf. Fig. 4. By contrast, the $\boldsymbol{a}$-axis lattice parameter, which is determined by intrastack interactions between adjacent TMTTF molecules, remains practically unaffected by the transition at T_{CO}. It therefore seems reasonable to include the anions and their coupling to the TMTTF molecules in the discussion of the CO process. In Fig. 4, we propose a simple scheme, which is to involve the charge degrees of freedom on the TMTTF stacks and their coupling to the anions. Upon cooling through T_{CO}, the charge ρ on the TMTTF molecule changes from a homogeneous distribution with $\rho = 0.5$ (in units of e) above T_{CO} to a modulated structure which alternates by $\pm\delta$ along the TMTTF stacks below. For deriving the resulting 3D charge pattern, we start by considering a stack of anions along the $\boldsymbol{a}$ axis and the two nearest-neighbor stacks of TMTTF molecules linked via short S-F contacts (green lines in Fig. 4). For a fixed charge modulation on one of the stacks, the electrostatic energy of the whole array can be reduced if one of the anions' nearest-neighbor TMTTF molecules is charge-rich $(TMTTF)^{(\rho_0+\delta)}$ (black symbols) and the other one charge-poor $(TMTTF)^{(\rho_0-\delta)}$ (white symbols), while the anions perform slight shifts towards the charge-rich ones. The resulting anion displacements (indicated by the arrows in Fig. 4), which are uniform for all anions and lift the inversion symmetry, together with the minimization of Coulomb energies of adjacent stacks along the $\boldsymbol{b}$ axis determine the 3D charge pattern unambiguously.

The importance of the anion potential for stabilizing the CO state in the $(TMTTF)_2X$ salts has been pointed out by several authors [6,8,11,26,27]. In Ref. [6], it was argued that, for small Peierls couplings, a sufficiently strong coupling to the anion displacement field can generate a $4k_F$

CO state accompanied by a uniform $\boldsymbol{q} = (q_{\parallel}, q_{\perp}) = (0, 0)$ displacement of the anions with respect to their symmetric positions. The latter state is consistent with the 3D displacement pattern proposed here.

The anomalies in α_i disclosed at T_{CO} are small and lack any indications for discontinuous changes of the lattice parameters, consistent with a second-order phase transition. A detailed analysis of the phase transition anomaly is, however, precluded by the anomalous background expansivity, although the rapid reduction of α_{c^*} immediately below T_{CO} indicates a slightly broadened steplike anomaly, i.e., a mean-field-type transition. This would in fact be expected at the CO transition as a result of long-range Coulomb forces and clearly revealed by the Curie-Weiss dependence of ϵ' [11].

Yet, as pointed out above, the CO transition appears to significantly affect the overall $\boldsymbol{c}^*$-axis expansivity, as T_{CO} roughly coincides with the temperature below which the negative contribution to α_{c^*} is no longer active. The process involved may be appreciated within the ''rigid-unit mode'' scenario proposed here to account for this negative α contribution: Above T_{CO}, CO fluctuations, evident from the dielectric measurements [11] to persist up to high temperatures, cause, via S-F contacts, positional fluctuations of the anions towards their new off-center equilibrium positions. These positional fluctuations may provide an effective damping of the anions' rigid-unit modes. Upon cooling through T_{CO}, the CO becomes static, giving rise to a freezing of these modes and, with it, a disappearance of the negative contribution to α.

Finally, we comment on the peak anomaly at T_{int} in β/T which is likely a phase transition related to the CO state. Possible scenarios may include disorder-related (relaxor) effects (at either T_{CO}, T_{int}, or both) or two consecutive transitions associated with different CO patterns. Arguments in favor of the latter possibility can be derived from infrared spectra for both salts [28] suggesting qualitative changes in the CO state below T_{int} and the sharpness of the anomalies in α_{c^*} observed here. On the other hand, ferroelectricity arising from a neutral-ionic type of transition akin to that discussed for TTF-chloranil [29] cannot be ruled out. Here the transition occurs over a wide temperature range with an onset expected to be a third-order transition [29].

In conclusion, the mysterious CO transition coupled to ferroelectricity in $(TMTTF)_2PF_6$ and $(TMTTF)_2AsF_6$ has been explored by using high-resolution thermal expansion measurements. The study reveals for the first time evidence for lattice effects accompanying the transition, thereby solving the long-standing puzzle surrounding this hitherto-called *structureless* transition. Based on the directional dependence of the observed effects, we propose a scheme involving the CO along the TMTTF stacks and its coupling to anion X^- displacements. The proposed uniform anion shifts, locking the charge modulation of adjacent TMTTF stacks, determine the 3D charge pattern unambiguously. The mechanism involved, being similar to the scenario discussed for the Wigner crystallization in $(DI\text{-}DCNQI)_2Ag$ [3], highlights the intricate role of the lattice degrees of freedom for stabilizing a CO ground state in a wide class of materials.

[1] M. Imada *et al.*, Rev. Mod. Phys. **70**, 1039 (1998); A. H. Castro Neto and C. Morais Smith, in *Strong Interactions in Low Dimensions*, edited by D. Baeriswyl and L. Degiorgi (Kluwer, Dordrecht, 2004).
[2] H. Seo and H. Fukuyama, J. Phys. Soc. Jpn. **75**, 051009 (2006).
[3] T. Kakiuchi *et al.*, Phys. Rev. Lett. **98**, 066402 (2007).
[4] D. Jérome, Chem. Rev. **104**, 5565 (2004).
[5] H. Seo and H. Fukuyama, J. Phys. Soc. Jpn. **66**, 1249 (1997).
[6] J. Riera and D. Poilblanc, Phys. Rev. B **63**, 241102(R) (2001).
[7] R. T. Clay *et al.*, Phys. Rev. B **67**, 115121 (2003).
[8] S. Brazovskii *et al.*, Synth. Met. **137**, 1331 (2003).
[9] D. S. Chow *et al.*, Phys. Rev. Lett. **85**, 1698 (2000).
[10] F. Nad *et al.*, Phys. Rev. B **62**, 1753 (2000).
[11] P. Monceau *et al.*, Phys. Rev. Lett. **86**, 4080 (2001).
[12] R. Laversanne *et al.*, J. Phys. Lett. **45**, L393 (1984).
[13] J.-P. Pouget and S. Ravy, J. Phys. I (France) **6**, 1501 (1996).
[14] P. Foury-Leylekian *et al.*, Physica (Amsterdam) **312B**, 574 (2002).
[15] R. Pott and R. Schefzyk, J. Phys. E **16**, 444 (1983).
[16] M. de Souza *et al.*, Phys. Rev. Lett. **99**, 037003 (2007).
[17] Measurements along the **a** axis for $X = AsF_6$ failed because the crystals cleaved as soon as a small stress was exerted by the dilatometer—an effect which is assigned to the highly 1D character of this salt.
[18] In Ref. [19], results on an interstack expansion coefficient on a different $X = PF_6$ crystal were given. The present results on well-oriented crystals suggest the data in Fig. 1 of Ref. [19] to be composed of contributions from $\alpha_{b'}$ and α_{c^*}, indicating some misalignment of the crystal studied there.
[19] M. Lang *et al.*, J. Phys. IV (France) **114**, 111 (2004).
[20] M. Dumm *et al.*, Phys. Rev. B **61**, 511 (2000).
[21] A. Brühl *et al.*, Phys. Rev. Lett. **99**, 057204 (2007).
[22] Substitution of PF_6 by Br, corresponding to an increase of pressure, raises J/k_B from 420 to 500 K [20].
[23] V. J. McBrierty *et al.*, Phys. Rev. B **26**, 4805 (1982).
[24] A. K. A. Pryde *et al.*, J. Phys. Condens. Matter **8**, 10 973 (1996); G. Ernst *et al.*, Nature (London) **396**, 147 (1998).
[25] F. Nad and P. Monceau, J. Phys. Soc. Jpn. **75**, 051005 (2006).
[26] W. Yu *et al.*, Phys. Rev. B **70**, 121101(R) (2004).
[27] J.-P. Pouget *et al.*, J. Low Temp. Phys. **142**, 147 (2006).
[28] M. Dumm *et al.*, J. Phys. IV (France) **131**, 55 (2005).
[29] J. Hubbard and J. B. Torrance, Phys. Rev. Lett. **47**, 1750 (1981).